Supporting Information

Controllable preparation of Eu^{3+} doped octacalcium phosphate and fluorescence study of its hydrolysis into hydroxyapatite

Heng Zhou, [a] *Jia Chen,* [a] *Xinyu Tan,* [a] *Xuanhe Wei,* [a] *Yingchao Han,* *[a]

[a] *State Key Laboratory of Advanced Technology for Materials Synthesis and Processing, Biomedical Materials and Engineering Research Center of Hubei Province, Wuhan University of Technology, Wuhan 430070, P.R. China*

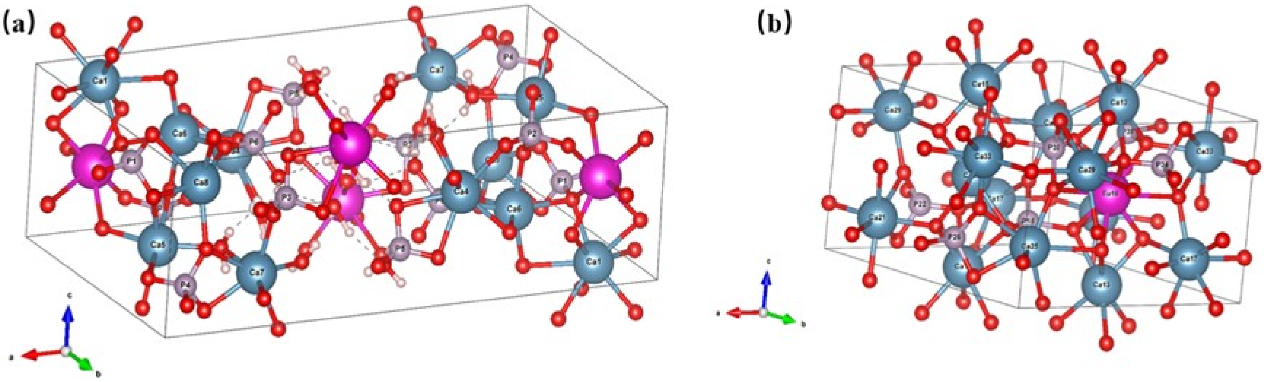

Scheme S1. Crystal structures of Eu-OCP(a) and Eu-HAP(b)

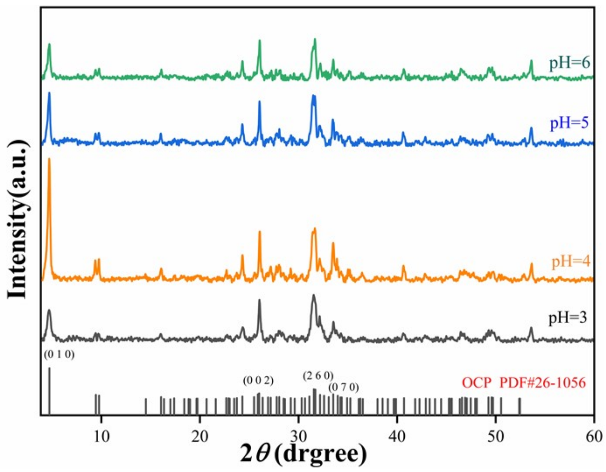

Figure S1. XRD patterns of OCP prepared at different pH

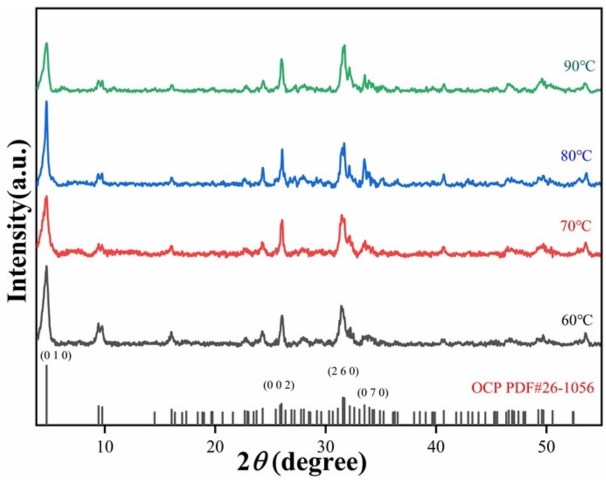

Figure S2. XRD patterns of OCP prepared at different temperatures

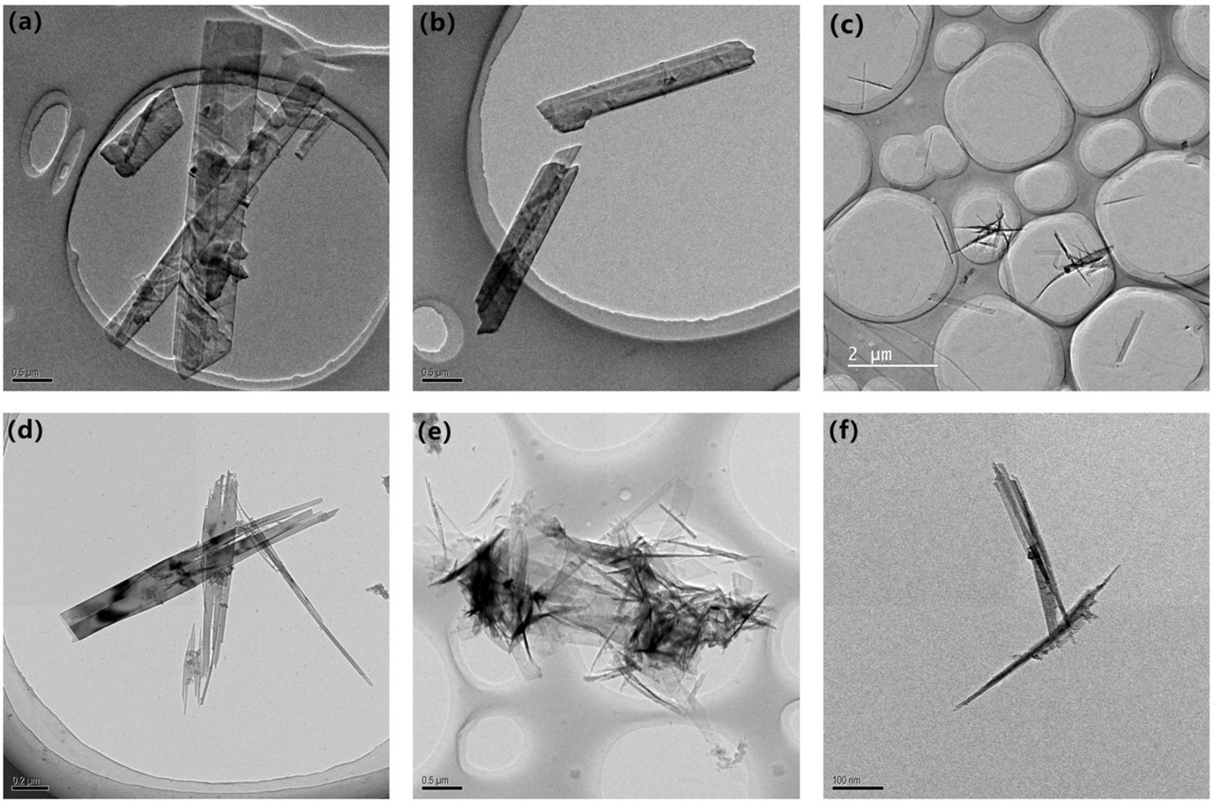

Figure S3. TEM images of OCP (a), Eu-OCP: 1% Eu (b), Eu-OCP: 2% Eu (c), Eu-OCP: 3% Eu (d), Eu-OCP: 4%Eu (e), Eu-OCP: 5%Eu (f)

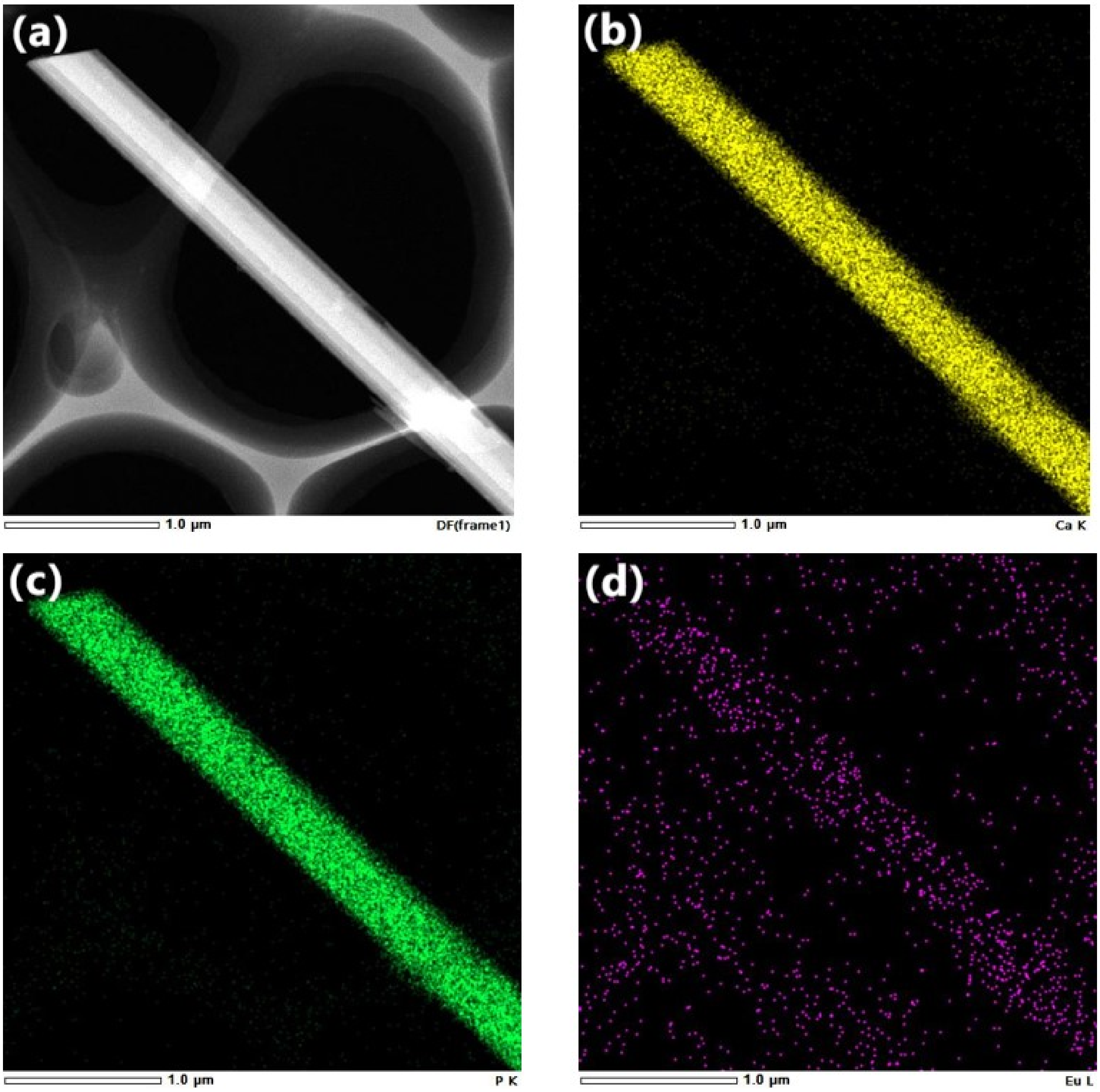

Figure S4. Topography (a), Ca elemental distribution (b), P elemental distribution (c) and Eu elemental distribution (d) of Eu-OCP

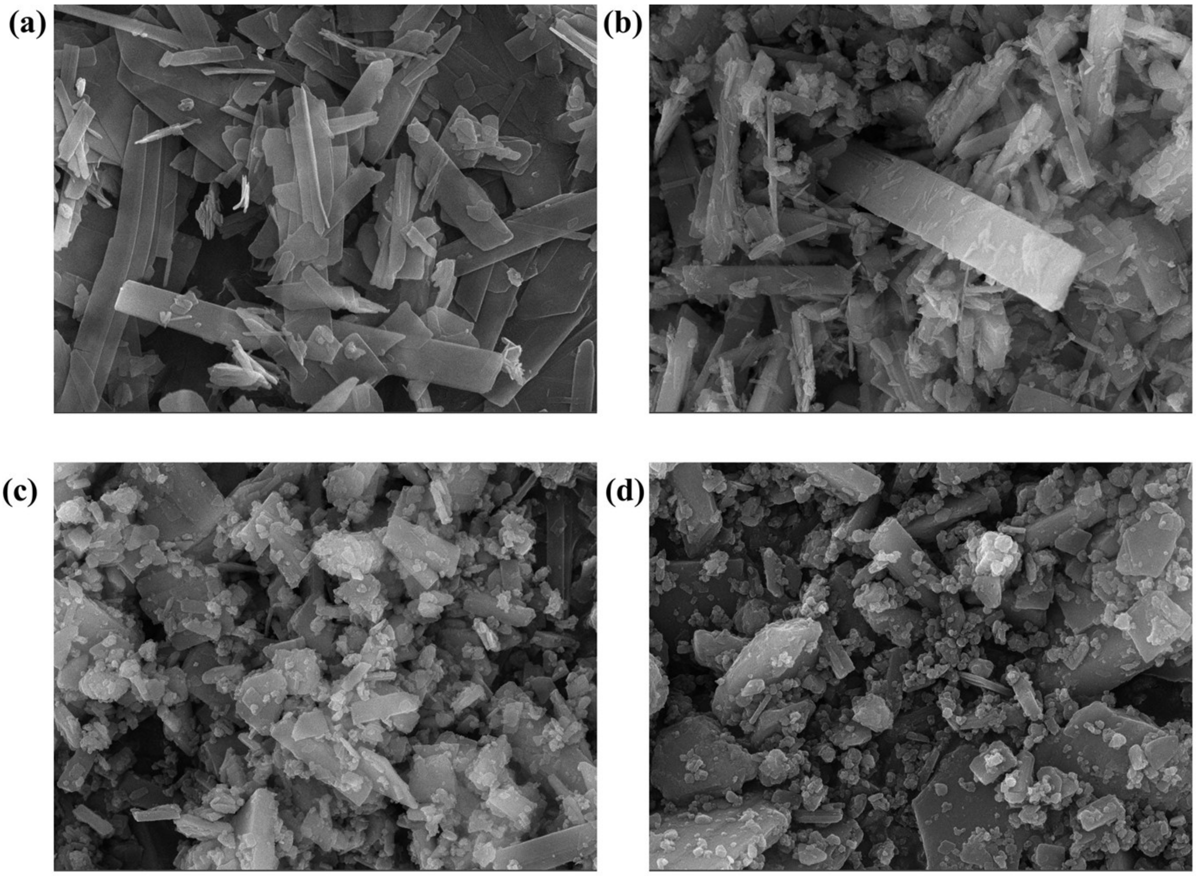

Figure S5. SEM images of OCP (a), Eu-OCP: 1% Eu (b), Eu-OCP: 3% Eu (c), Eu-OCP: 5%Eu (d)

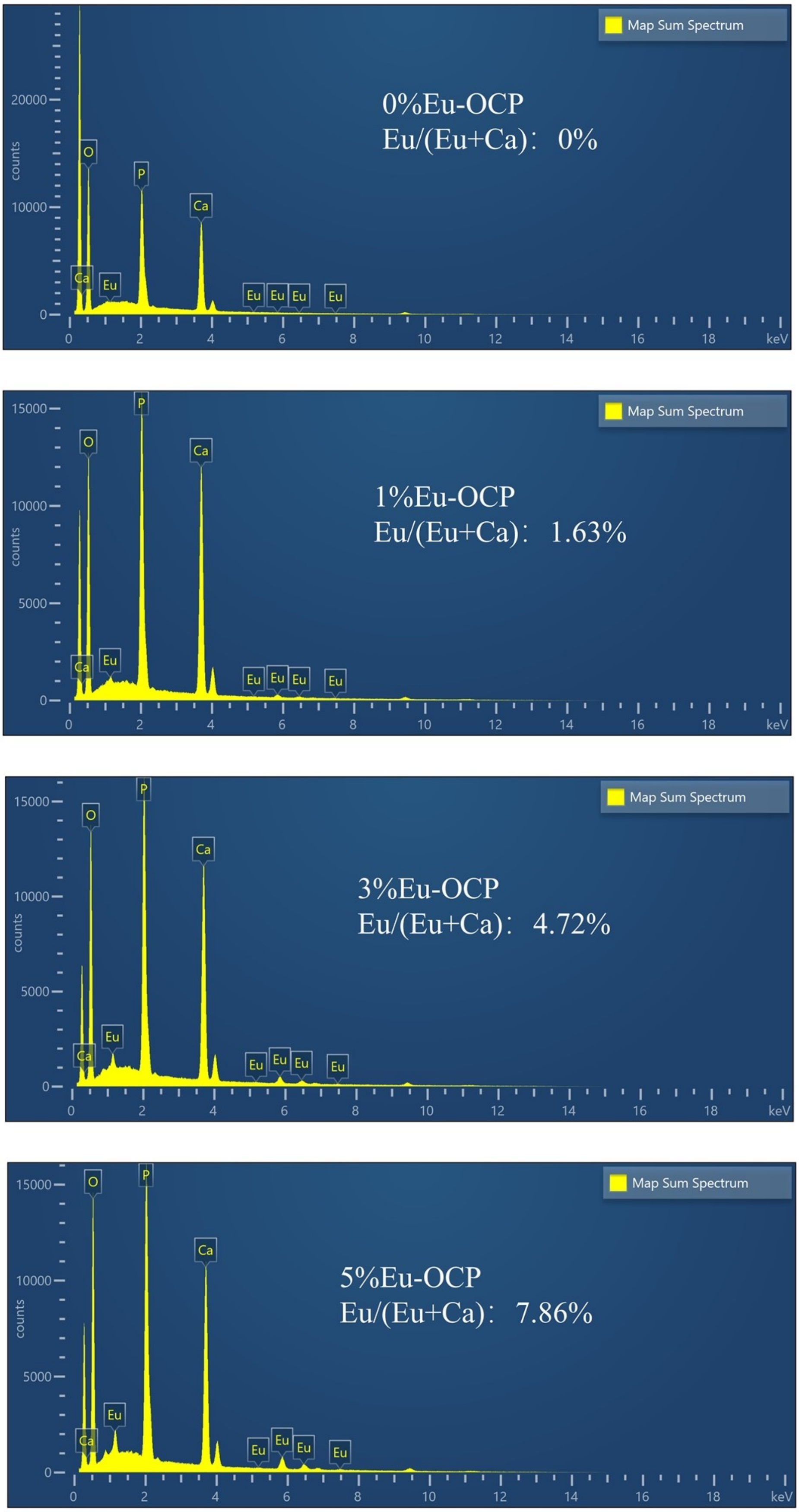

Figure S6. Eu-OCP SEM-EDX spectra with different Eu^{3+} doping ratios

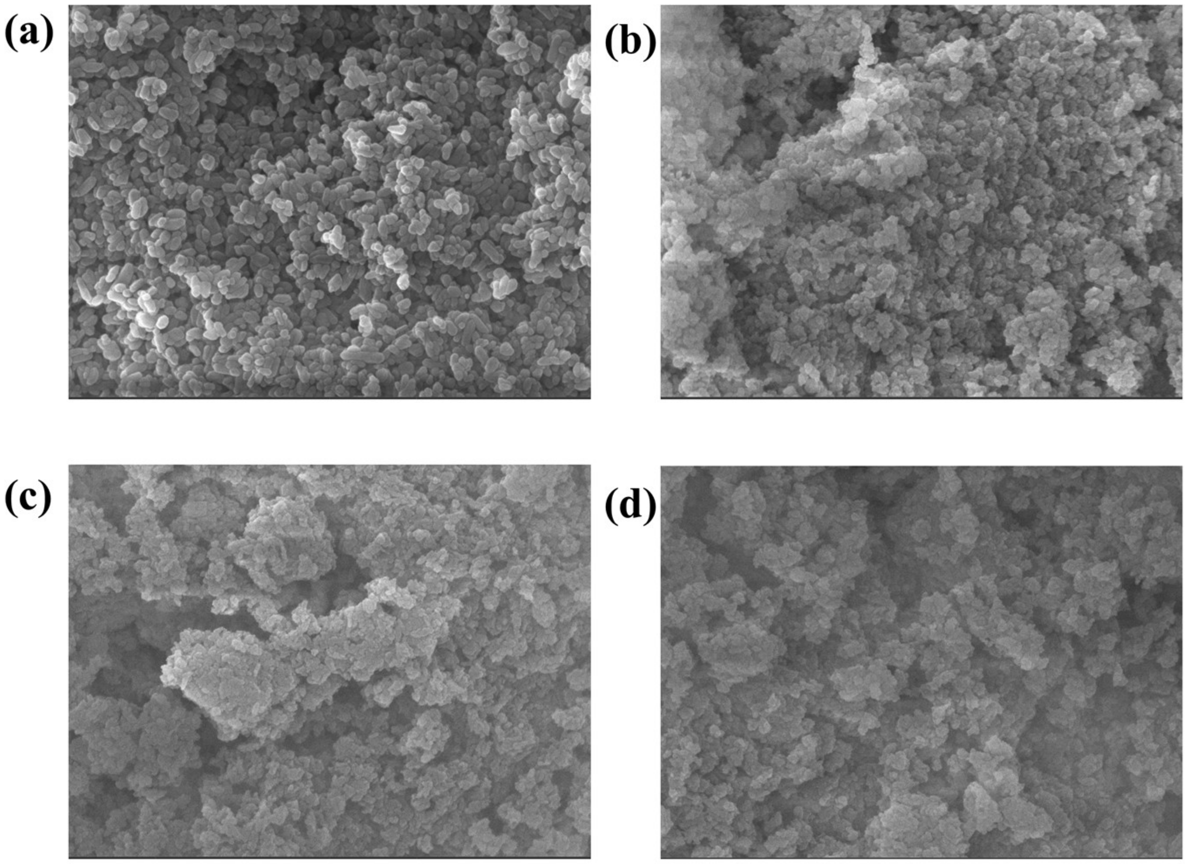

Figure S7. SEM images of HAP (a), Eu- HAP: 1% Eu (b), Eu- HAP: 3% Eu (c), Eu- HAP: 5%Eu (d)

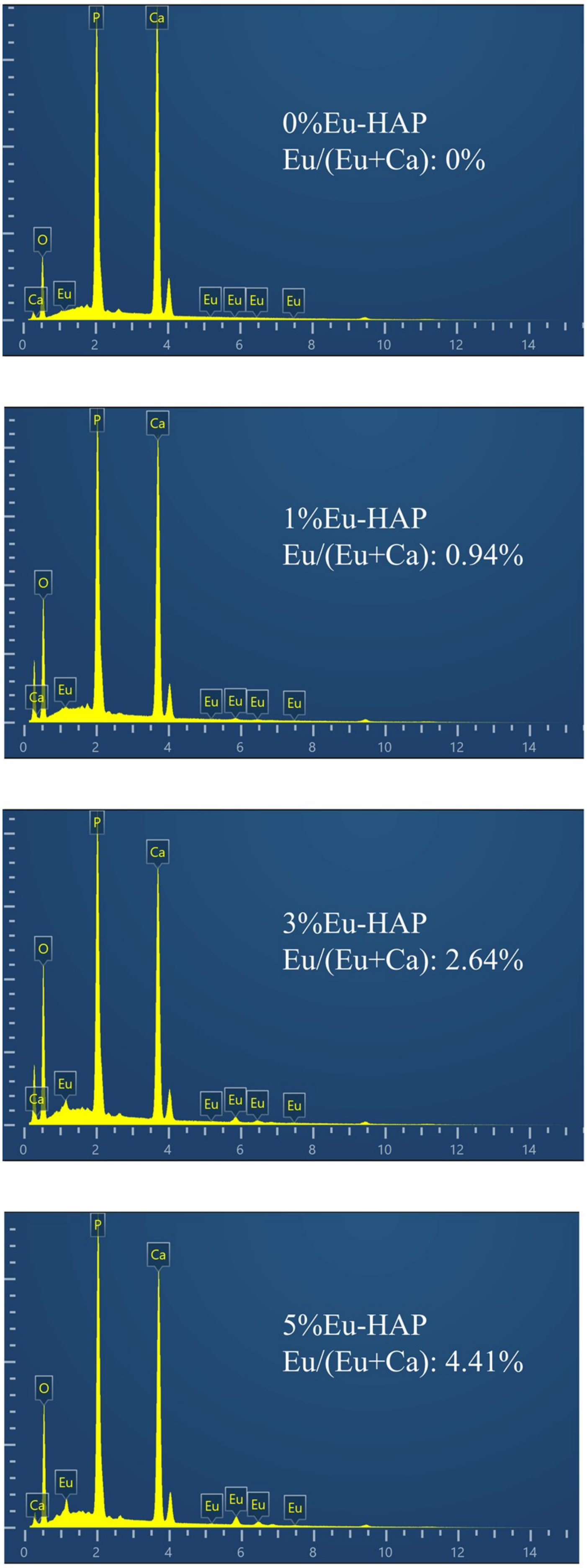

Figure S8. Eu-HAP SEM-EDX spectra with different Eu^{3+} doping ratios

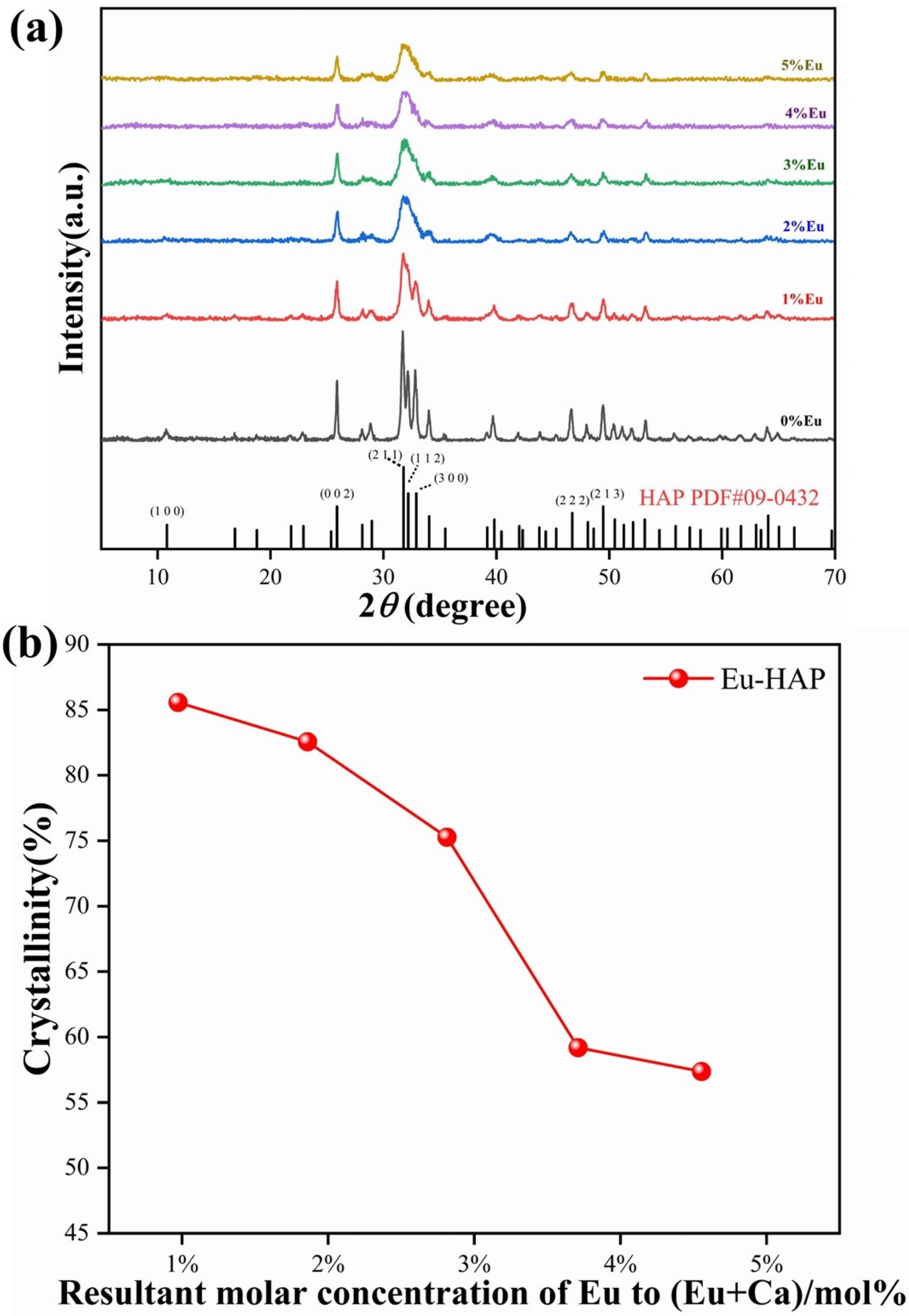

Figure S9. XRD spectra (a) and crystallinity variation (b) of Eu-HAP with different doping ratio

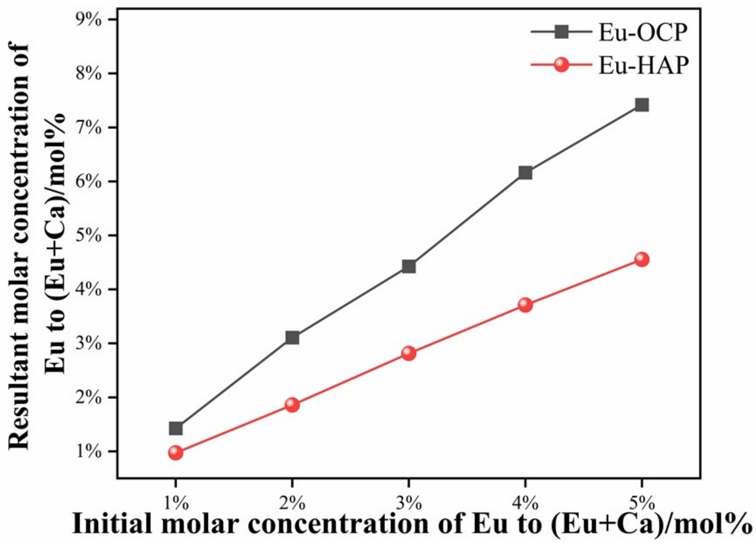

Figure S10. The variation of Eu/(Eu+Ca) molar ratio with the initial molar ratio of Eu/(Eu+Ca)

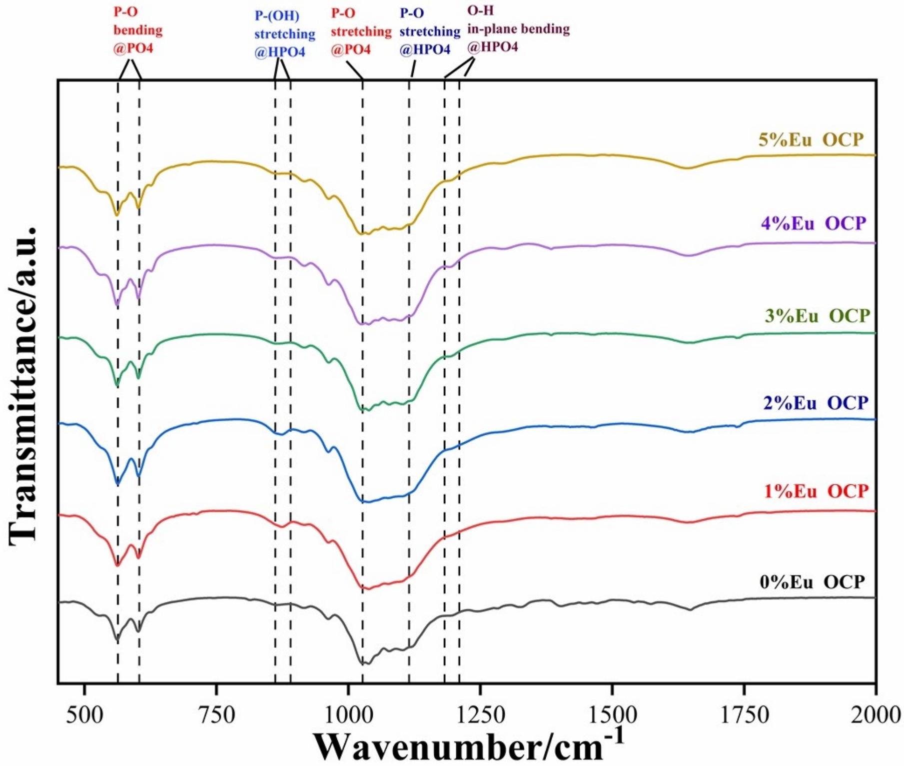

Figure S11. FT-IR spectra of Eu-OCP with different doping ratio

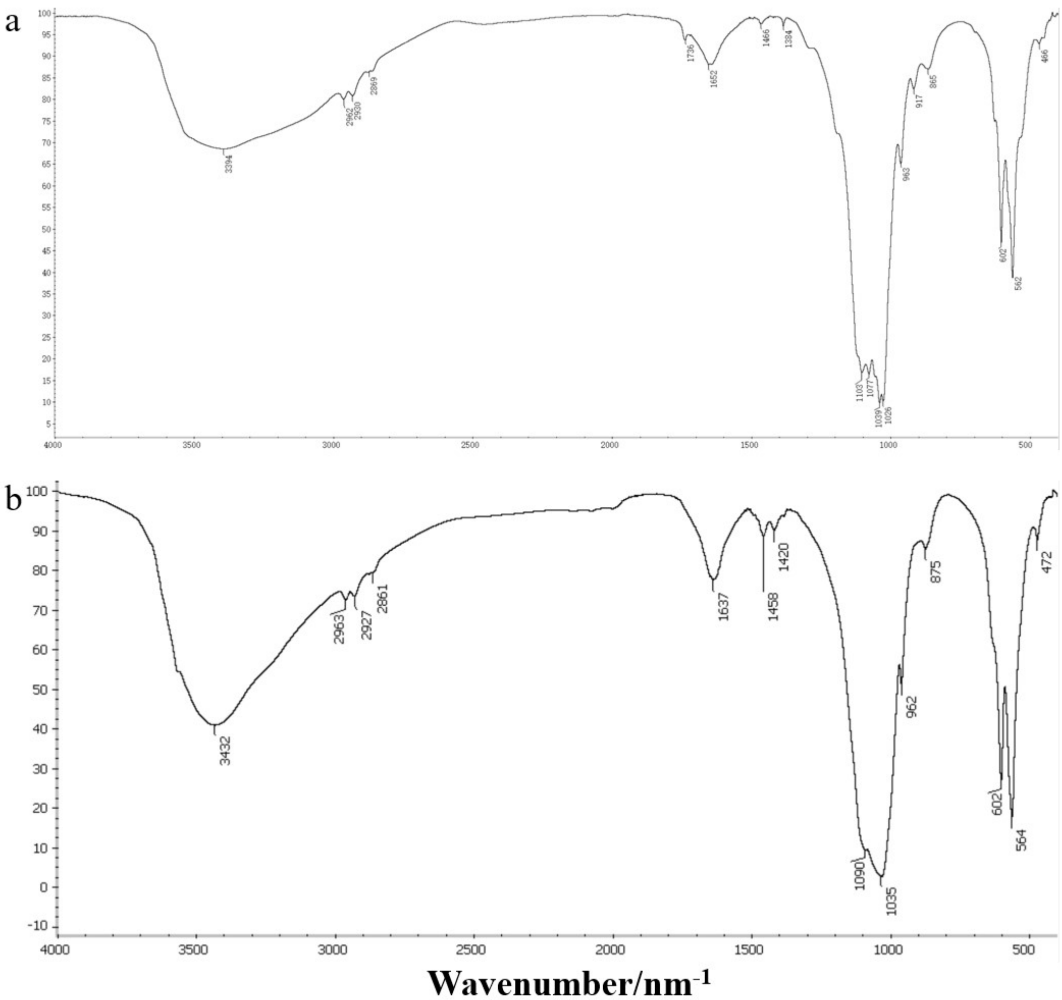

Figure S12. FT-IR spectra of Eu-OCP(a) and Eu-HAP(b)

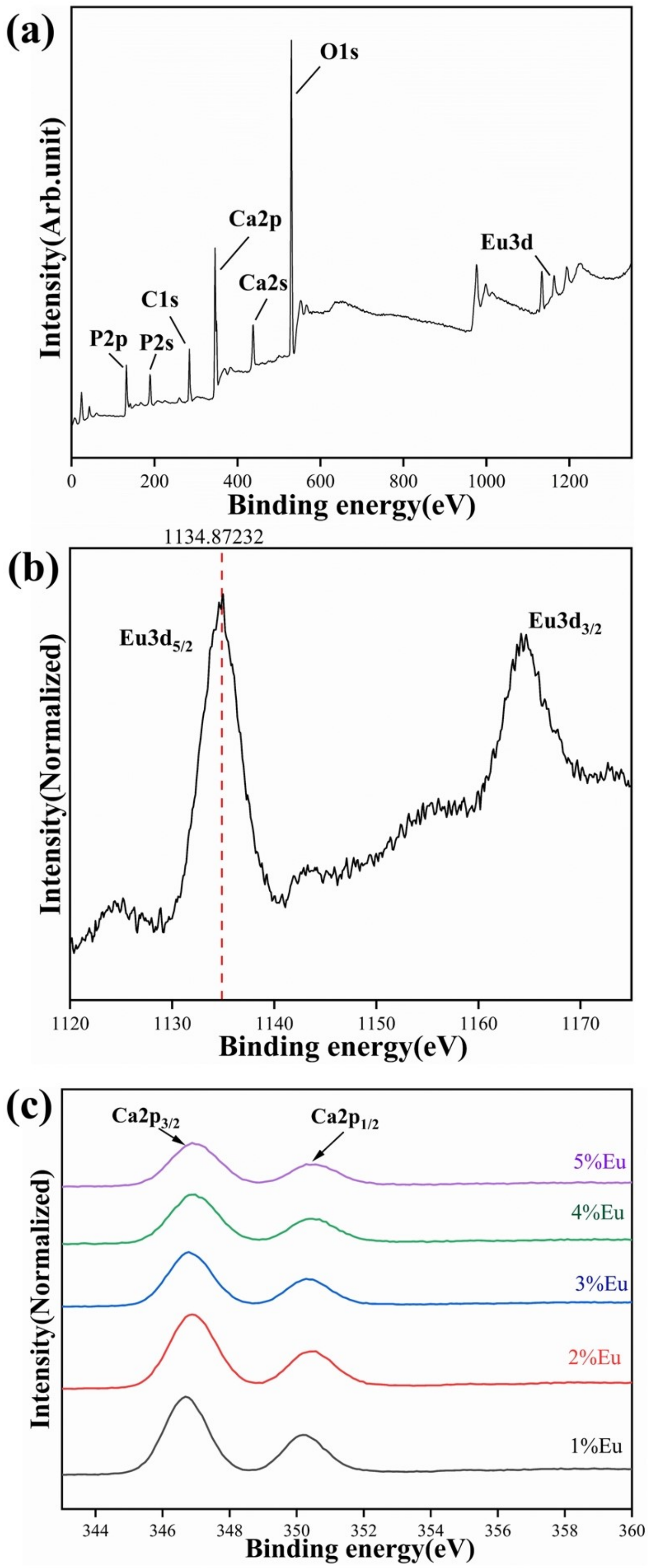

Figure S13. XPS full scan spectra of Eu-OCP surface (a), XPS spectra of Eu3d (b), XPS spectra of different doped ratios of Ca2p in Eu-OCP (c)

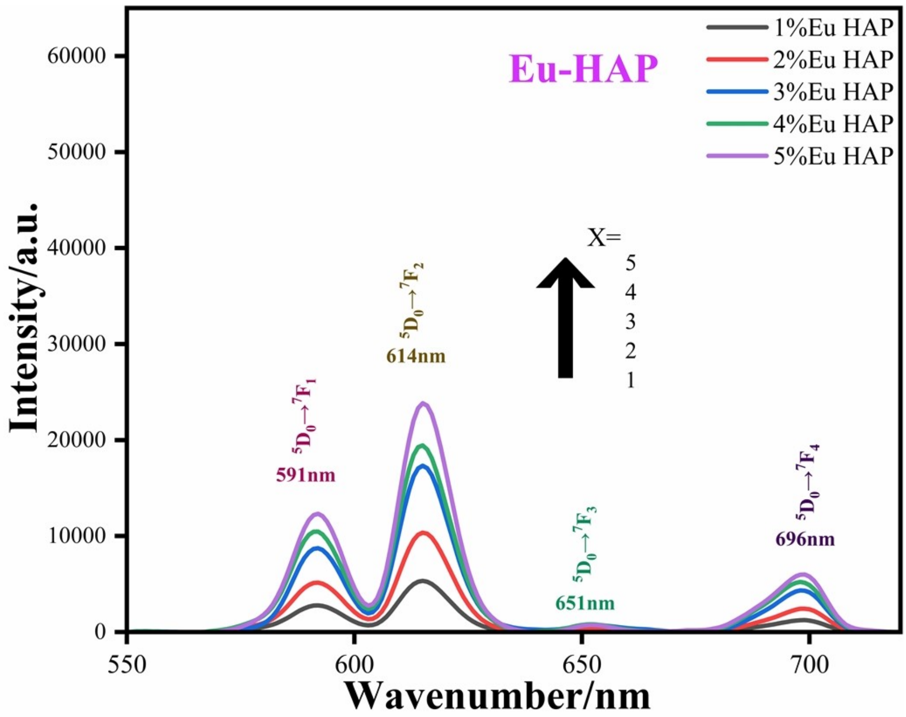

Figure S14. Fluorescence intensity changes of Eu-HAP

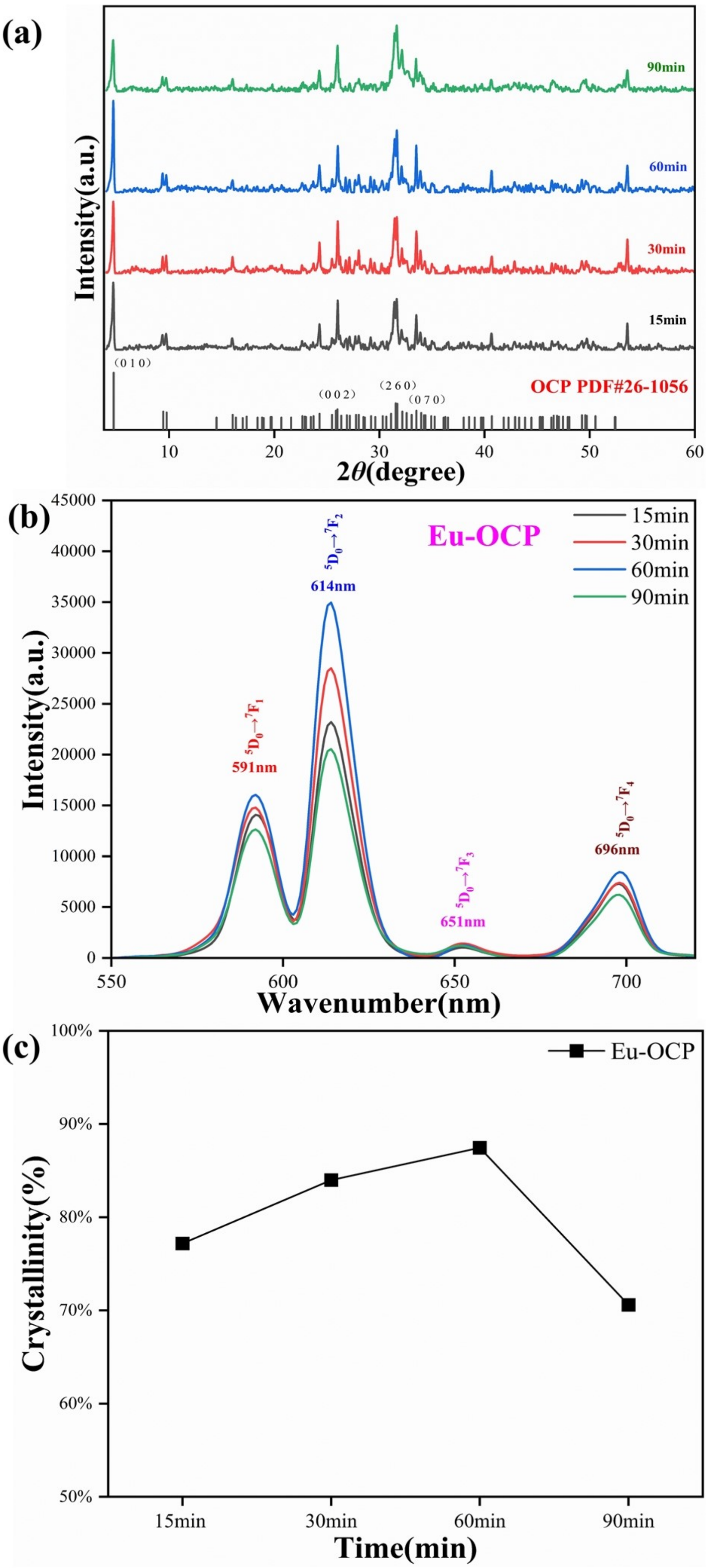

Figure S15. XRD spectra of Eu-OCP synthesized with 3% doping ratio at different titration times (a), fluorescence intensity spectra (b), crystallinity variation (c)

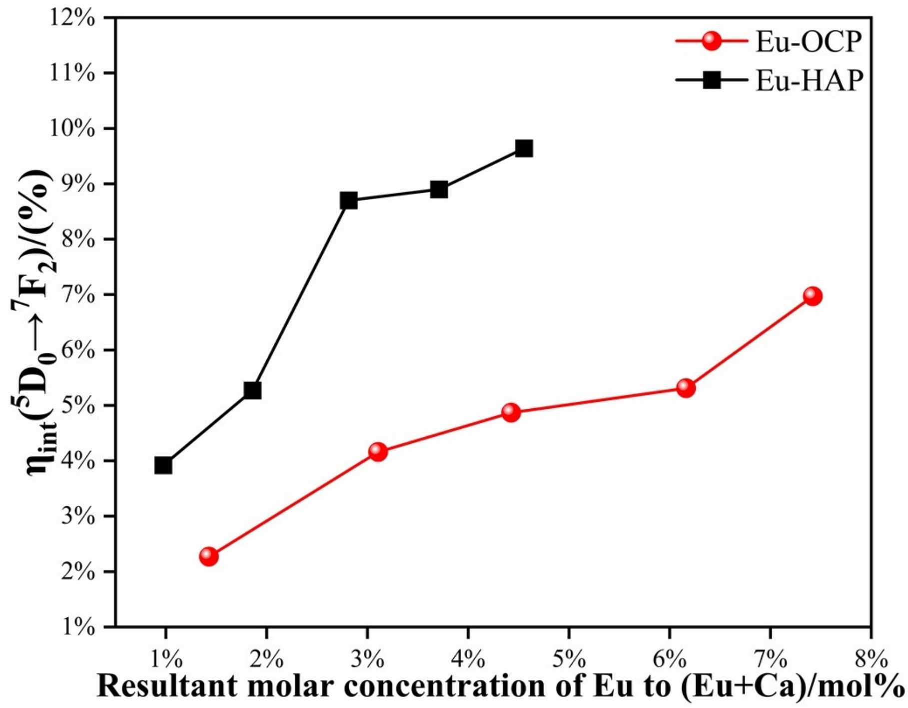

Figure S16. Quantum yields of Eu-OCP and Eu-HAP

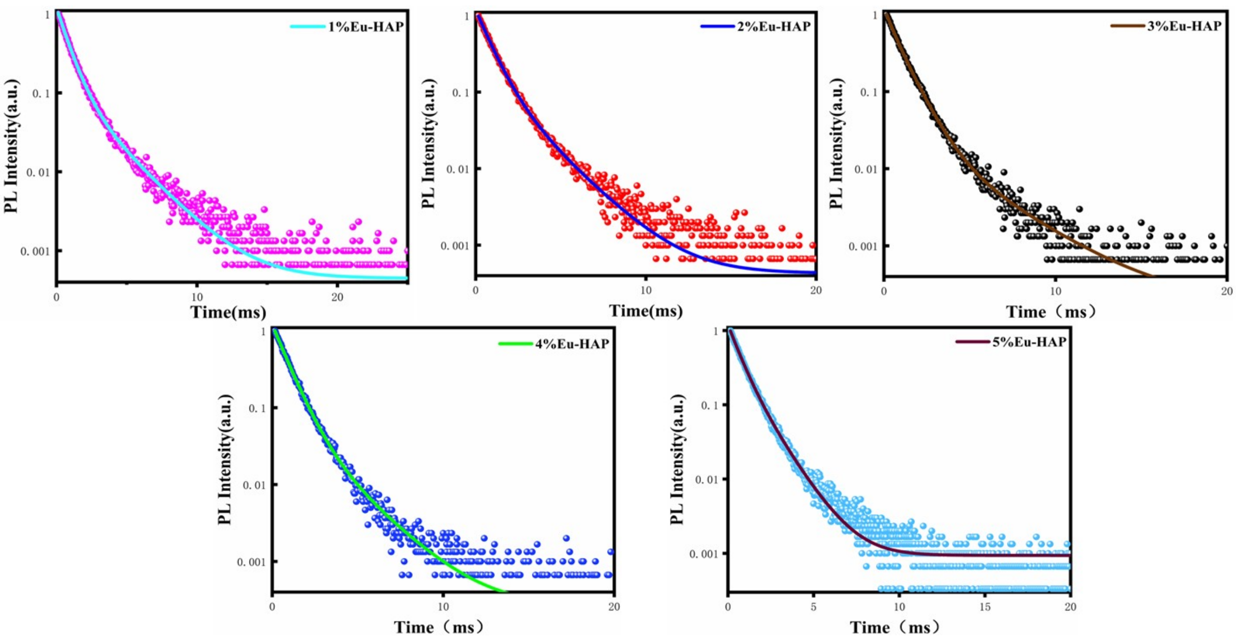

Figure S17. Changes in fluorescence lifetime of Eu-HAP with different doping ratios

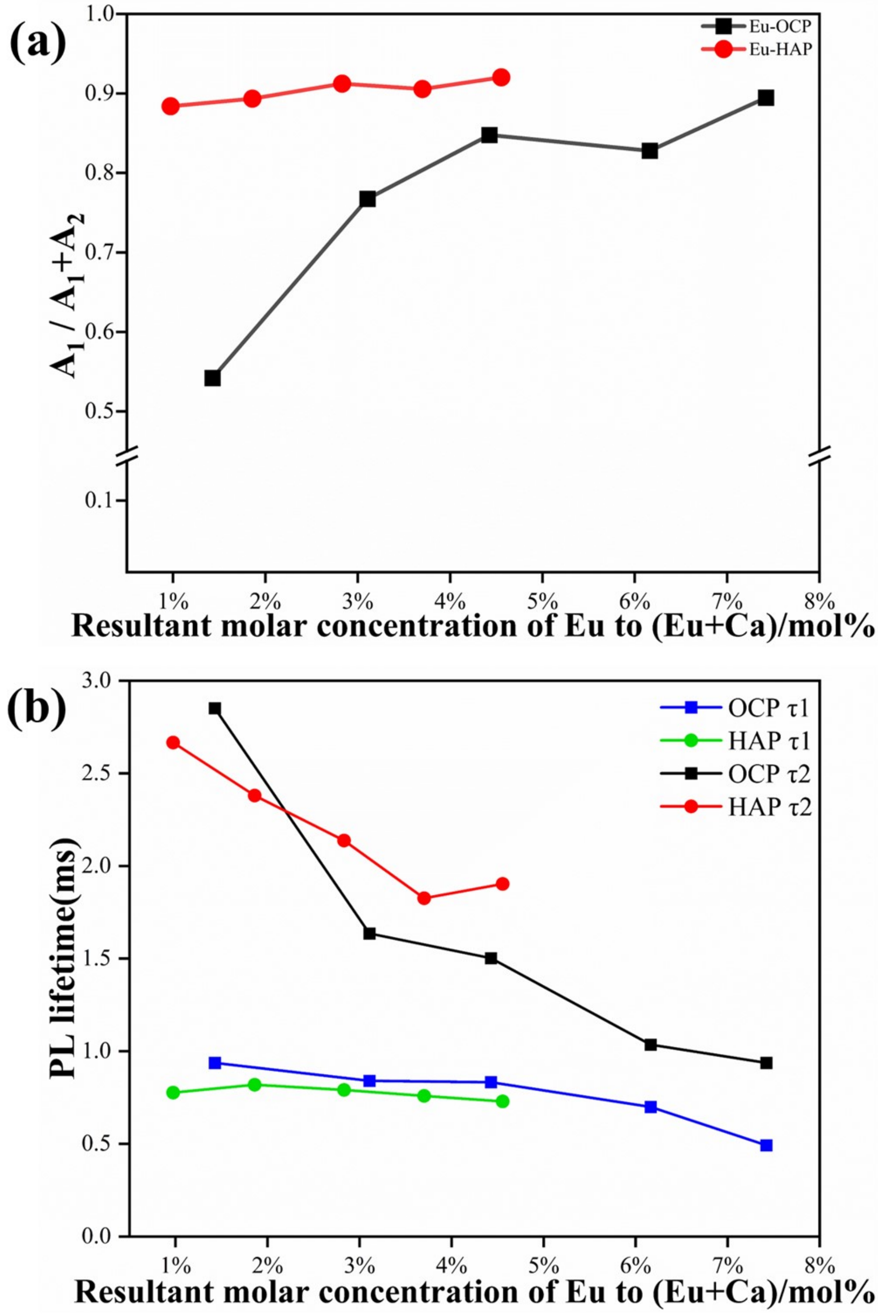

Figure S18. Variation of different doping ratios $A_1/(A_1+A_2)$ (a) and τ_1, τ_2 fluorescence lifetimes (b)

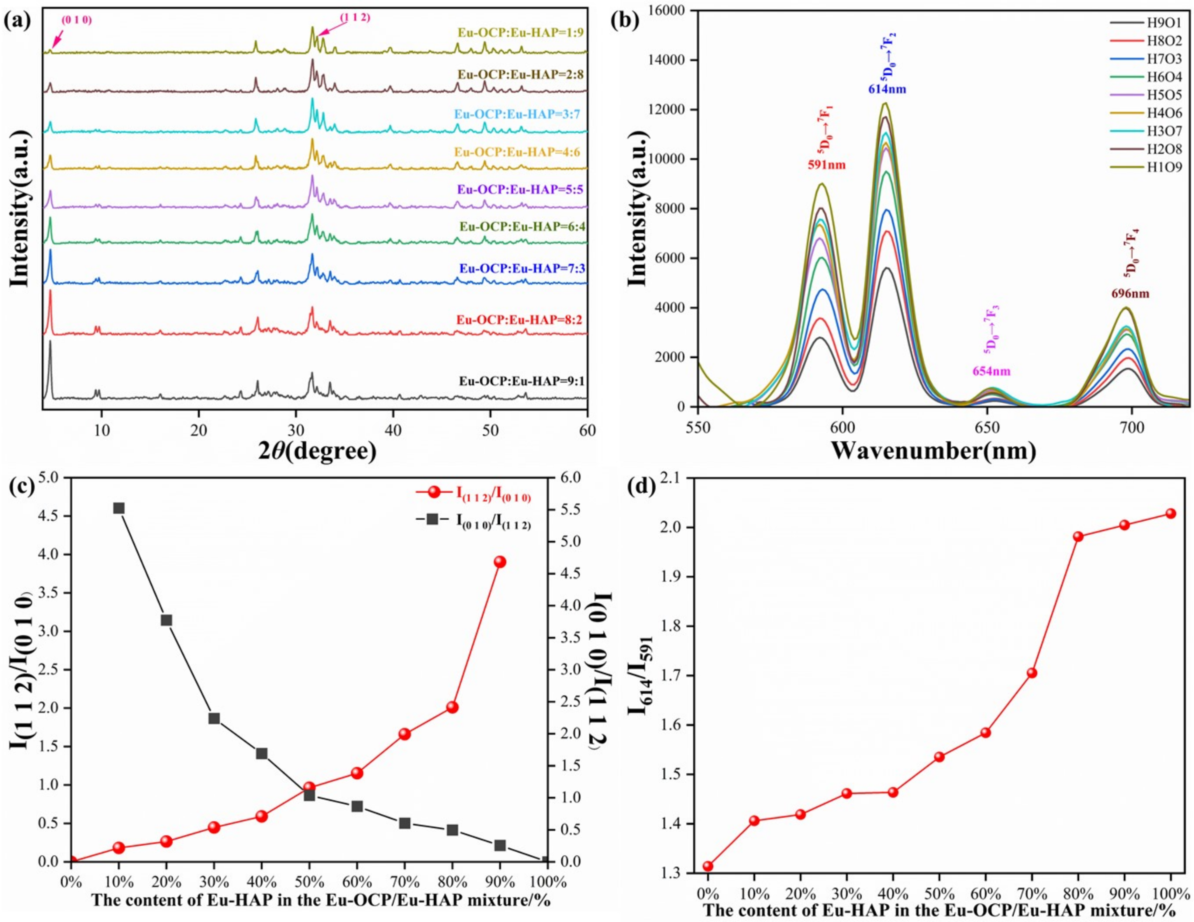

Figure S19. XRD spectra (a), fluorescence spectra (b) of different ratios of Eu-OCP blended with Eu-HAP. I $_{(1\ 1\ 2)}$/I $_{(0\ 1\ 0)}$ and I $_{(0\ 1\ 0)}$/I $_{(1\ 1\ 2)}$ (c) and I_{614}/I_{591} (d) with the ratio of Eu-HAP in the blending compound

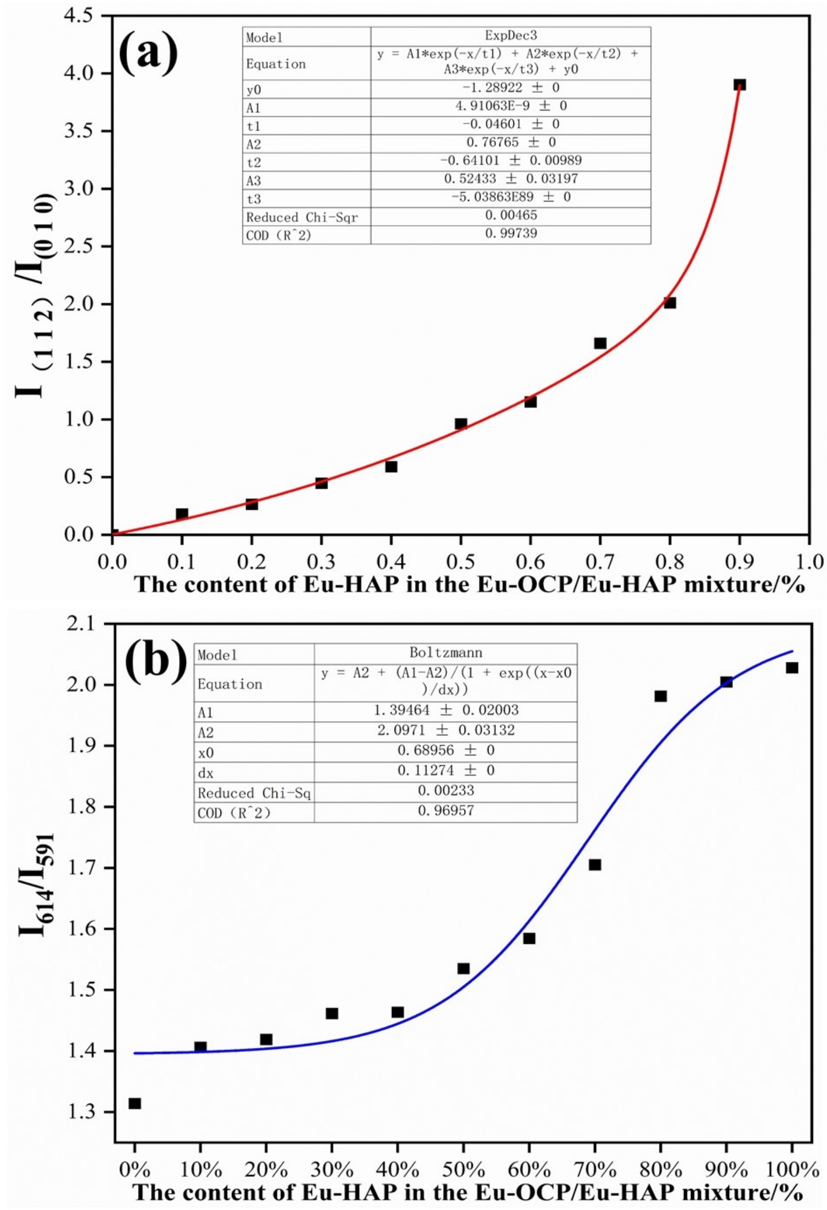

Figure S20. Fitting curves of $I_{(1\ 1\ 2)}/I_{(0\ 1\ 0)}$ (a) and I_{614}/I_{591} (b) to the Eu-HAP content in the blending system

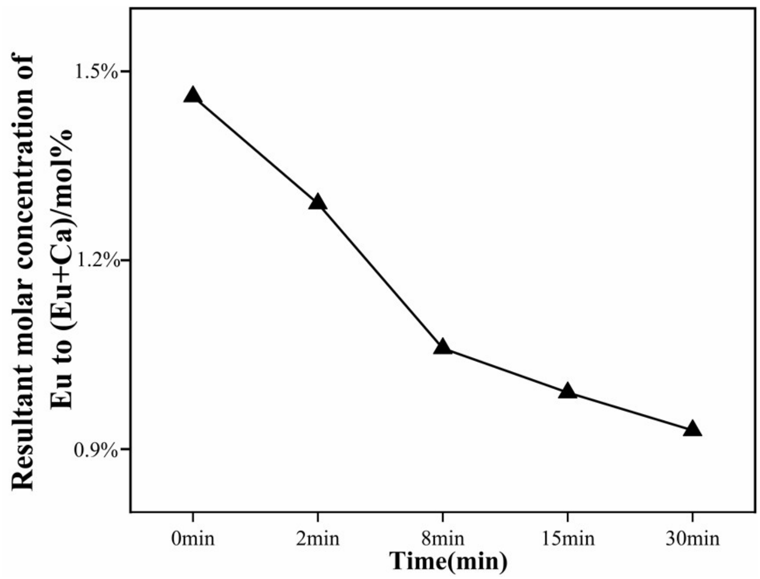

Figure S21. Resultant Eu/(Eu+Ca) molar ratio of mixtures at different hydrolysis time points